

However, these kinds of measurement results and estimation processes can be used further mRFID antenna design and real applications.

#### 4. CONCLUSION

In this article, measured read range of 900-MHz-band mRFID system has been presented. We show a relationship between the RFID reader antenna gains and possible read ranges. The measured read range results are compared with calculated read range. In most cases, the measured read range data and calculated estimation data are fairly close with  $\pm 10\%$  variation. Based on the calculated data curves, we can estimate the proper reader antenna gain to satisfy the desirable read range. The results of mRFID read range test with various antennas, and read range estimation are useful for future research and application of mRFID.

#### REFERENCES

1. K. Finkenzerler, RFID Handbook, 2nd ed., John Wiley, West Sussex, England, 2003.
2. J. Siden, P. Jonsson, T. Olsson, and G. Wang, Performance degradation of RFID system due to distortion in RFID tag antenna, In: 2001 International Conference on Microwave and Telecommunication Technology, pp. 371–373.
3. L. Ukkonen, D. Engles, L. Sydanheimo, and M. Kivikoski, Planar wire-type inverted-F RFID tag antenna mountable on metallic objects, In: 2004 International Symposium on Antennas and Propagation and USNC/USRI National Radio Science Meeting, vol. 1, June 2004, pp. 101–104.
4. A. Delichatsios, et al., Folded microstrip patch-type RFID tag antenna mounted on a box corner, In: 2006 International Symposium on Antennas and Propagation and USNC/USRI National Radio Science Meeting, vol. 1, July 2006, pp. 3213–3216.
5. P.V. Nikitin and K.V.S. Rao, Measurement of backscattering from RFID tags, In: Proceedings of the 2005 Antenna Measurement Techniques Association, Oct. 2005, New Port, RI, USA, vol. 1, pp. 300–303.
6. P.V. Nikitin and K.V.S. Rao, Performance Limitations of passive UHF RFID systems, In: 2006 International Symposium on Antennas and Propagation and USNC/USRI National Radio Science Meeting, vol. 1, June 2006, pp. 1011–1014.
7. V. Pillai, Impedance matching in RFID tags: to which impedance to match? In: 2006 International Symposium on Antennas and Propagation and USNC/USRI National Radio Science Meeting, vol. 1, June 2006, pp. 3505–3508.

© 2007 Wiley Periodicals, Inc.

## COMPACT DESIGNS OF A BAND-PASS FILTER WITH NOVEL OPEN-LOOP RESONATORS

Xin-Hua Jiang and Guo-Hui Li

School of Communication and Information Engineering, Shanghai University, Shanghai 200072, China; Corresponding author: rrrrecluse@hotmail.com

Received 23 April 2007

**ABSTRACT:** In this article, several square open-loop resonators with transmission lines are proposed to design the optimized bandpass filters. A compact microstrip filter using an open-loop resonator was designed, fabricated and measured. At the center frequency  $f_0 = 1.80$  GHz, a 3-dB bandwidth of 5% can be varied from 1.76 to 1.85 GHz. The filter shows a maximum insertion loss in passband of 0.1 dB. A transmission zero is realized at about 3.1 GHz, and the attenuation at this frequency exceeds 70 dB. When compared with the conventional filters using cou-

pled square open-loop resonators, the proposed filter has a size reduction of 30%. Good agreement between measurements and simulations are obtained. © 2007 Wiley Periodicals, Inc. Microwave Opt Technol Lett 49: 2755–2757, 2007; Published online in Wiley InterScience (www.interscience.wiley.com). DOI 10.1002/mop.22837

**Key words:** miniaturization; bandpass filter; open-loop resonator; microstrip

#### 1. INTRODUCTION

The development of very compact microwave filters with printed circuit board (PCB) fabrication technologies is of great interest for the miniaturization. So far, much work has been done to develop a variety of compact bandpass filters. In Ref. [1], a bandpass filter was designed by cascading a highpass filter and a lowpass filter, where one is equivalently embedded into the other, so that the circuit area of entire circuit can be greatly saved. In Refs. [2, 3], miniature filters using srr/csrr structures were proposed by employing the distributed capacitance between concentric rings. On the basis of the concept of electromagnetic bandgaps (EBGs) [4] and defected ground structure (DGS) [5], numerous studies have been done to the slow-wave characteristics of these structures in a wide variety of microwave circuits, which have the advantages of compact size. A compact narrow-band bandpass filter has been proposed [6], which consists of two identical microstrip open-loop resonators with coupled and crossing lines. This kind of filters has miniaturized dimensions and two deep notches in the stopband.

In this article, a compact bandpass filter using novel open-loop resonators is proposed. When compared with the conventional filters using square open-loop resonators, the bandpass filter owns its practical advantages: it has low insertion losses in the passband, high-frequency selectivity, and reduced area of circuit layout.

#### 2. FILTER DESIGN

##### 2.1. Novel Resonators and Their Electromagnetic Characteristics

The novel resonators are shown in Figures 1(a)–1(c). Each one consists of a square open-loop with transmission lines directly connected to it. Compared with the conventional open-loop resonator [Fig. 1(d)], these structures efficiently employ the space inside the loop and they do not occupy extra space, resulting in size reduction. It is noted that the four square loops possess the same dimensions. Because of the capacitive loading, these resonators have lower resonator frequencies when compared with the conventional open-loop resonator [Fig. 1(d)]. The resonant frequencies of the four structures are compared as shown in Figure 2. As can be seen in Figure 2, the resonant frequencies of the proposed structures are 1.80, 2.02, and 2.26 GHz, respectively, whereas that of the conventional one in Figure 1(d) is 2.56 GHz, which means that the proposed resonators have a more size reduction.

First, let us consider the capacitively loaded lossless transmission line resonator of Figure 3, where  $C_L$  is the loaded capacitance;  $Z_a$ ,  $\beta_a$ , and  $d$  are the characteristic impedance, the propagation

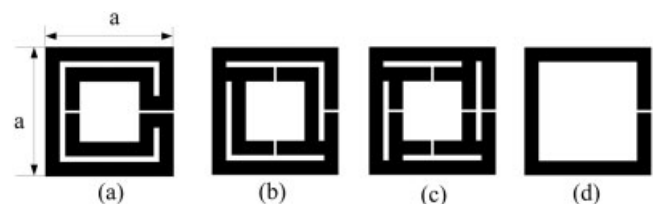


Figure 1 Four different resonators

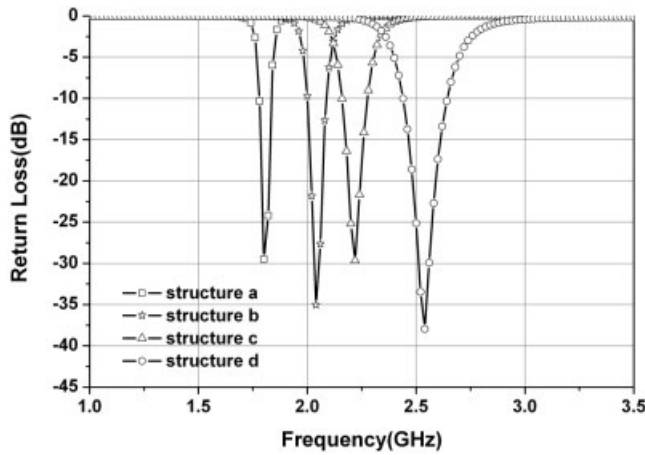


Figure 2 Return loss for four resonators

constant, and the length of the unloaded line, respectively. By calculating ABCD parameter matrix, we obtain [7]:

$$\theta_{a0} = 2 \tan^{-1} \left( \frac{1}{\pi f_0 Z_a C_L} \right) \quad (1)$$

$$\theta_{a1} = 2\pi - 2 \tan^{-1} (\pi f_1 Z_a C_L) \quad (2)$$

It can clearly be seen that from (1) and (2) that  $\theta_{a0} = \pi$  and  $\theta_{a1} = 2\pi$  when  $C_L = 0$ . This is the case for the unloaded half-wavelength resonator. For  $C_L \neq 0$ , it can be shown that the resonant frequencies decline. The ratio of the first spurious resonant frequency to the fundamental one  $f_1/f_0$  increases with the loading capacitance, resulting in size reduction and wide stopband.

### 2.2. Filter Design

As a demonstration, a compact narrow bandpass filter is designed using resonator (a) in Figure 1. The substrate with relative dielectric constant of 2.8 and a thickness of 0.8 mm is used for this design. Figure 4(a) shows the filter configuration. On comparison, a conventional square open-loop filter is also designed, shown in Figure 4(b). The dimension of the loops in Figure 4(a) are the same with that in Figure 4(b). The resonant frequencies of the two structures are compared as shown in Figure 2.

After an optimally design process, the dimensions of the proposed structures are chosen as follows:

$a = 12$  mm;  $b = 12$  mm;  $w = 2$  mm;  $n = 2$  mm;  $m = 0.4$  mm;  $k = 0.2$  mm;  $s = 0.2$  mm;  $p = 1$  mm.

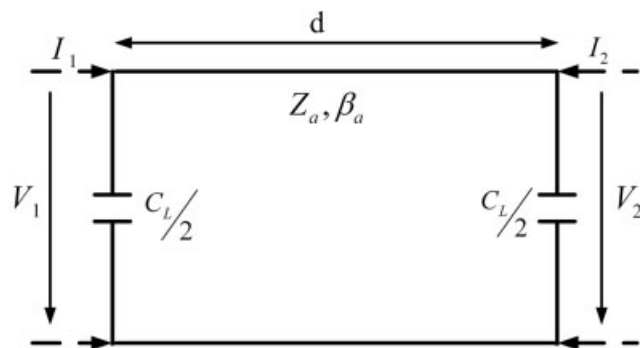


Figure 3 Capacitively loaded transmission line resonator

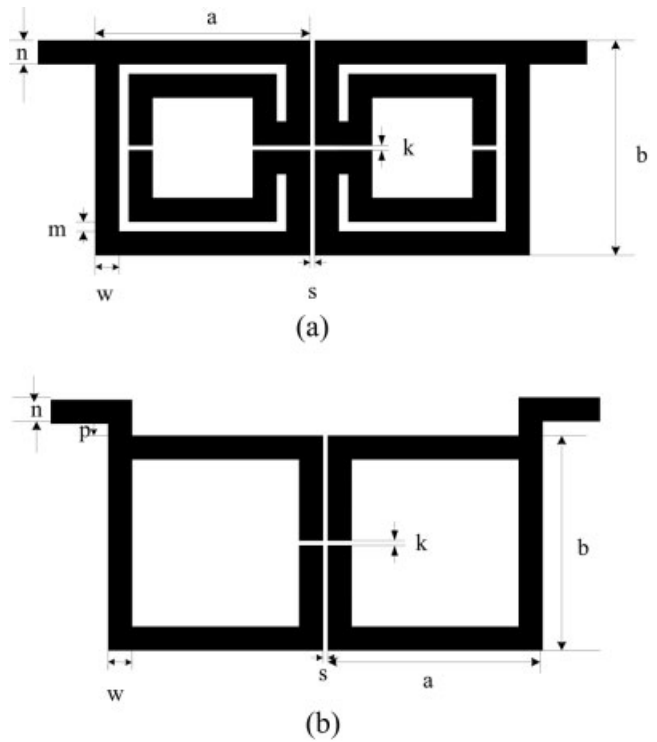


Figure 4 Geometry of two types of filters(a)proposed structure(b)conventional structure

### 3. SIMULATION AND MEASUREMENT

The simulations for structure a [Fig. 4(a)] and structure b [Fig. 4(b)] were carried out using an EM Simulator, sonnet EM. The simulation results are summarized in Table 1.

Where  $f_0$  is the center frequency of bandpass filter,  $S_{21max}$  is the maximal attenuation,  $BW_{20dB}$  is stopband width (20 dB), and selectivity  $\xi$  [8]:

$$\xi = \frac{\alpha_{min} - \alpha_{max}}{f_s - f_c} \text{ (dB/GHz)} \quad (3)$$

where  $\xi$  is selectivity in dB/GHz;  $\alpha_{max}$  and  $\alpha_{min}$  are 3 dB attenuation point and 20 dB attenuation point, respectively;  $f_c$  and  $f_s$  are their stopband frequency and cut-off frequency, respectively. It should be noted that, we use  $\alpha_{min} = S_{21max} = 14.4$  dB in Eq. (3) instead of 20 dB as proposed for the conventional filter. At the center frequency of 1.80 GHz, the fabricated filter has a 3 dB bandwidth of 5%, ranging from 1.76 to 1.85 GHz. The maximum insertion loss in passband is 0.1 dB. A transmission zero is realized at about 3.1 GHz, and the attenuation at this frequency exceeds 70 dB. We can obtain good stopband characteristic with 20dB stopband from 2.0 to 3.5 GHz. Compared with the conventional filters using coupled square open-loop resonators, the center frequency of this novel bandpass filter has shifted from 2.56 to 1.80 GHz, meaning a size reduction of 30%. A photograph of the fabricated

TABLE 1 Comparison Between Two Types of Filters

	Filter of Type a	Filter of Type b
$f_0$ (GHz)	1.80	2.56
$S_{21max}$ (dB)	-70	-14.4
$\xi$ (dB/GHz)	64.7	10.6
$BW_{20dB}$ (GHz)	1.5	0

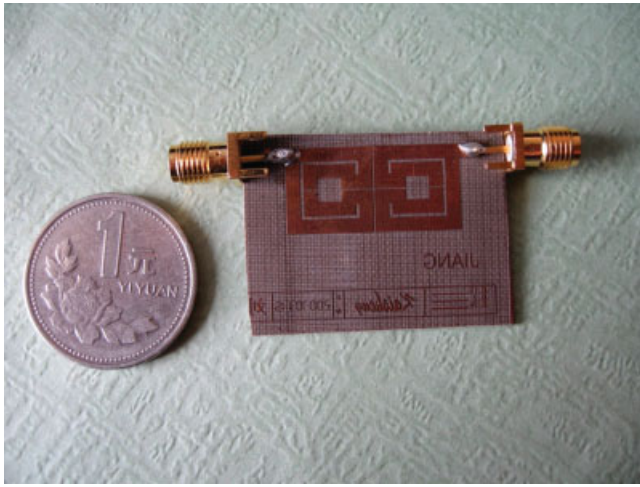


**Figure 5** The fabricated filter. [Color figure can be viewed in the online issue, which is available at [www.interscience.wiley.com](http://www.interscience.wiley.com)]

filter is shown in Figure 5. The filter is measured by using an Agilent8722ES network analyzer. Figure 6 shows the simulated and measured results of the proposed bandpass filter, where [M] denotes the measurements and [S] denotes the simulations. The measured results agree well with the simulated ones. The insertion loss of measurement is a little bigger than that of simulation. The main reasons are the fabrication tolerance of the filter and the incomplete homogeneous dielectric substrate.

#### 4. CONCLUSION

In this article, three novel resonators with capacitive loading have been proposed. A compact narrow bandpass filter is designed and fabricated using one of these novel resonators. The filter has a compact size, which is 30% smaller than the conventional filters using square open loop. Simulation and measurement on the fabricated filter show high-frequency selectivity and good stop-band characteristic. The measured results agree well with the simulations.

#### ACKNOWLEDGMENTS

This work was supported by the Development Fund of the Shanghai Education Committee (No. 2006AZ034) and partly supported by the Shanghai Leading Academic Disciplines (No. T0102).

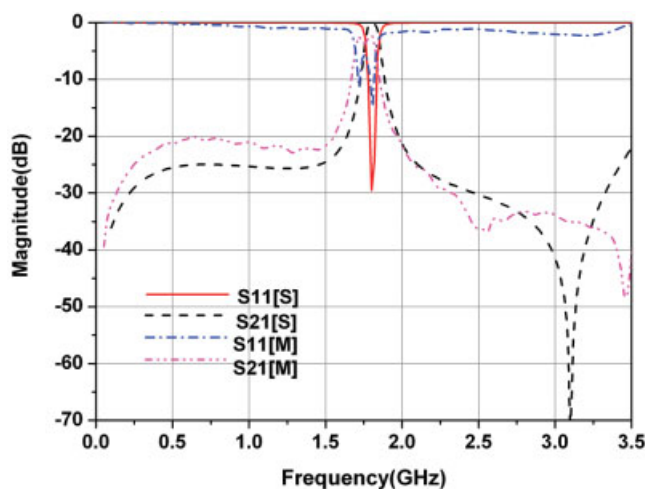


**Figure 6** Simulated and measured results. [Color figure can be viewed in the online issue, which is available at [www.interscience.wiley.com](http://www.interscience.wiley.com)]

#### REFERENCES

1. C.-L. Hsu, F.-C. Hsu, and J.-T. Kuo, Microstrip bandpass filters for ultra-wideband (UWB) wireless communications, *IEEE MTT-S Long Beach, CA* (2005), 679–682.
2. J. Bonache, F. Martin, F. Falcone, et al., Application of complementary split-ring resonators to the design of compact narrow band-pass structures in microstrip technology, *Microwave Opt Tech Lett* 46 (2005), 508–511.
3. J. García-García, F. Martín, F. Falcone, et al., Microwave filters with improved stopband based on sub-wavelength resonators, *IEEE MTT* 53 (2005), 1997–2006.
4. L.F. Falcone et al., Compact photonic bandgap microstrip structure, *Microwave Opt Tech Lett* 23 (1999), 233–236.
5. J.I. Park, J. Yun, and D. Ahn, Design of the novel coupled-line bandpass filter using defected ground structure with wide stopband performance, *IEEE MTT* 50 (2002), 2037–2043.
6. X.-Y. Zhang, J.-X. Chen, and X. Quan, Compact passband filter using open-loop resonators with capacitive loading, *Microwave Opt Tech Lett* 49 (2007), 83–84.
7. J.S. Hong and M.J. Lancaster, *Microstrip filters for RF/microwave applications*, Wiley, New York, 2001, pp. 392–396.
8. N.C. Karmaker, Improved performance of photonic bandgap microstrip line structures with the use of Chebyshev distributions, *Microwave Opt Tech Lett* 33 (2002), 1–5.

© 2007 Wiley Periodicals, Inc.

## MULTI-BAND RECTANGULAR MICROSTRIP ANTENNAS

Amit A. Deshmukh<sup>1</sup> and K. P. Ray<sup>2</sup>

<sup>1</sup> MPSTME, NMIMS (DU), Vile-Parle, Mumbai 400056, India;

Corresponding author: [amitdeshmukh76@yahoo.com](mailto:amitdeshmukh76@yahoo.com)

<sup>2</sup> SAMEER, I.I.T. Campus, Powai, Mumbai 400076, India

Received 31 March 2007

**ABSTRACT:** Configurations with slotted rectangular microstrip antennas using rectangular slot and half U-slot cut inside the patch for multi-band operation are proposed. Also, the multi-port network models for these multi-band rectangular microstrip antennas are proposed. © 2007 Wiley Periodicals, Inc. *Microwave Opt Technol Lett* 49: 2757–2761, 2007; Published online in Wiley InterScience ([www.interscience.wiley.com](http://www.interscience.wiley.com)). DOI 10.1002/mop.22880

**Key words:** multi-band rectangular microstrip antenna; multi-port network model; half U-slot; rectangular slot

#### 1. INTRODUCTION

Multi-band microstrip antenna (MSA) are realized by placing a shorting post or by cutting a slot at an appropriate position inside the patch or by placing an open or short circuit stub on the edges of MSA or by using active tunable elements [1–3]. When a nearly half or quarter wavelength slot is cut inside the MSA, it adds another resonant mode near the fundamental mode of the patch and gives the dual band response. In this article, dual band and triple band configurations are proposed, wherein a rectangular slot and half U-slot are cut inside the rectangular MSA (RMSA). Also, the multi-port network model (MNM) for these slotted RMSAs is proposed which gives the voltage distribution at all the frequencies. These RMSAs were first analyzed using IE3D software on glass epoxy substrate ( $\epsilon_r = 4.3$ ,  $h = 0.159$  cm, and  $\tan \delta = 0.02$ ) followed by MN modeling and experimental verification [4]. In these multi-band RMSAs, the feed point with probe diameter of